Cell

Resource

Quantitative Temporal Viromics: An Approach to Investigate Host-Pathogen Interaction

Michael P. Weekes,[1,3,4,*] Peter Tomasec,[2,4] Edward L. Huttlin,[1] Ceri A. Fielding,[2] David Nusinow,[1] Richard J. Stanton,[2] Eddie C.Y. Wang,[2] Rebecca Aicheler,[2] Isa Murrell,[2] Gavin W.G. Wilkinson,[2] Paul J. Lehner,[3] and Steven P. Gygi[1,*]
[1]Department of Cell Biology, Harvard Medical School, 240 Longwood Avenue, Boston, MA 02115, USA
[2]School of Medicine, Cardiff University, Tenovus Building, Heath Park, Cardiff CF14 4XX, UK
[3]Cambridge Institute for Medical Research, University of Cambridge, Hills Road, Cambridge CB2 0XY, UK
[4]Co-first author
*Correspondence: mpw1001@cam.ac.uk (M.P.W.), steven_gygi@hms.harvard.edu (S.P.G.)
http://dx.doi.org/10.1016/j.cell.2014.04.028

SUMMARY

A systematic quantitative analysis of temporal changes in host and viral proteins throughout the course of a productive infection could provide dynamic insights into virus-host interaction. We developed a proteomic technique called "quantitative temporal viromics" (QTV), which employs multiplexed tandem-mass-tag-based mass spectrometry. Human cytomegalovirus (HCMV) is not only an important pathogen but a paradigm of viral immune evasion. QTV detailed how HCMV orchestrates the expression of >8,000 cellular proteins, including 1,200 cell-surface proteins to manipulate signaling pathways and counterintrinsic, innate, and adaptive immune defenses. QTV predicted natural killer and T cell ligands, as well as 29 viral proteins present at the cell surface, potential therapeutic targets. Temporal profiles of >80% of HCMV canonical genes and 14 noncanonical HCMV open reading frames were defined. QTV is a powerful method that can yield important insights into viral infection and is applicable to any virus with a robust in vitro model.

INTRODUCTION

Human cytomegalovirus (HCMV) is a ubiquitous herpesvirus that persistently infects the majority of the world's population (Mocarski et al., 2013). Following primary infection, HCMV persists for the lifetime of the host under the control of a healthy immune system (Nichols et al., 2002). Reactivation from viral latency to productive infection in immunocompromised individuals, and acquisition of primary infection in utero or during transplantation can lead to serious disease (Mocarski et al., 2013). With the possibility of CMV being used as a vaccine vector (Hansen et al., 2013), a complete understanding of its ability to modulate host immunity is paramount.

During productive infection, HCMV gene expression is conventionally divided into immediate-early (IE), early (E), and late (L) phases. The *IE2* gene is primarily responsible for activating transcription of early-phase genes. By definition, early genes encode functions necessary to initiate viral DNA replication. Early-late genes (E-L) are initially transcribed at low levels and upregulated after the onset of viral DNA replication, whereas true-late genes are expressed exclusively after DNA replication and include proteins required for the assembly and morphogenesis of HCMV virions (Mocarski et al., 2013).

HCMV is a paradigm for viral immune evasion that perturbs the interferon (IFN) response (Powers et al., 2008), suppresses antigen presentation through the efficient downregulation of MHC class I (van der Wal et al., 2002), and has eight or more genes that act to suppress natural killer (NK) cell function (Wilkinson et al., 2008). Nevertheless, our understanding of how HCMV evades and modulates intrinsic immune sensors and effectors during infection remains superficial. It is not known which viral proteins are present at the cell surface, or how viral and host proteins are regulated during infection. Prior analysis of the temporal expression of HCMV genes has relied either on semiquantitative immunoblots of single viral proteins, or microarrays, which cannot capture posttranscriptional change (Ma et al., 2012). Although 604 noncanonical HCMV open reading frames (ORFs) have been identified by ribosomal footprinting (Stern-Ginossar et al., 2012), it is not yet clear how many of these ORFs encode functional polypeptides. Answering such questions has the potential to reveal mechanisms of immune evasion, cell-surface drug targets, and an improved understanding of HCMV biology.

In this paper, we describe a proteomic approach to study viral infection (quantitative temporal viromics, QTV), based on precise temporal quantitation of plasma membrane (PM) and intracellular proteins. We combined plasma membrane profiling, our recently described method for isolation of highly purified PM proteins for proteomic analysis (Weekes et al., 2012), with study of whole-cell lysates (WCL). We quantified proteins from up to ten samples using isobaric chemical tags (tandem mass tags, TMT) (McAlister et al., 2012) and MS3 mass spectrometry. This utilizes

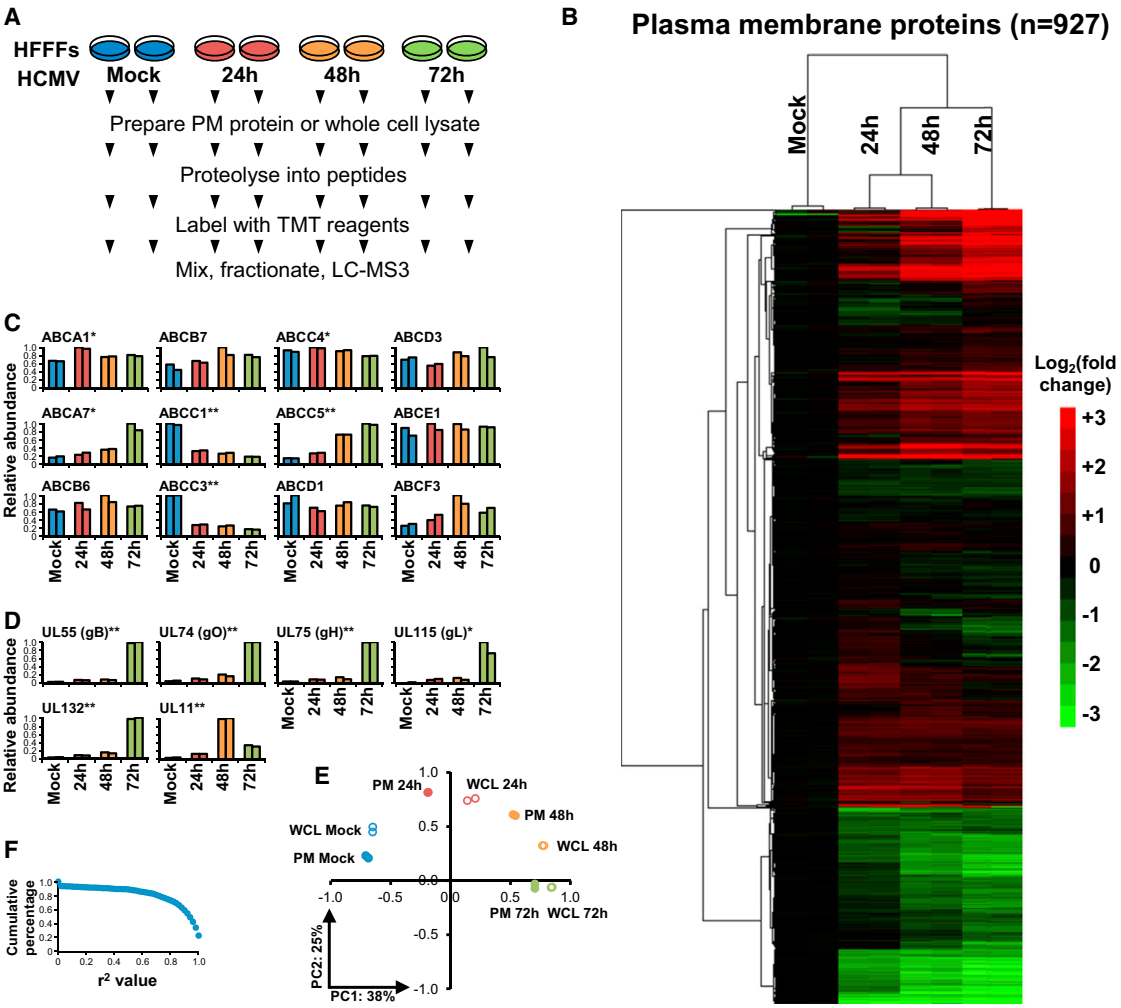

Figure 1. Temporal Plasma Membrane Profiling of HCMV-Infected Fibroblasts

(A) Workflow of experiments PM1 and WCL1.

(B) Hierarchical cluster analysis of all proteins quantified in experiment PM1 and annotated "plasma membrane," "cell surface," "extracellular," or "short GO" (Figure S1A).

(C) All ABC transporters quantified. One-way ANOVA with multiple hypothesis correction: *$p < 0.005$, **$p < 0.0001$.

(D) Quantitation of all HCMV proteins reported present at the surface of infected fibroblasts. gB, gH, gL, gO, and UL132 are virion envelope glycoproteins expressed late in infection. One-way ANOVA with multiple hypothesis correction: *$p < 0.005$, **$p < 0.0001$.

(E) Principal component analysis of all quantified proteins from experiments PM1 and WCL1 confirmed that biological replicates were highly reproducible and suggested that the major source of variability within a given experiment was duration of infection.

(F) Correlation between proteins quantified in experiments PM1 and PM2.

See also Figure S1 and Table S1.

two consecutive peptide fragmentation steps to liberate TMT reporters, minimizing interference from coisolated ions and enabling uniquely precise quantitative measurement of protein abundances at a near-global proteomic scale (Ting et al., 2011). We quantified >8,000 proteins including 1,184 cell-surface proteins and 81% of all canonical HCMV proteins over eight time points during productive infection, providing a near-complete temporal view of the host proteome and HCMV virome. Quantitative temporal viromics provides a framework for the study of any virus, enabling in-depth analysis of key aspects of viral pathogenesis.

RESULTS

Validation of Quantitative Temporal Viromics

We infected primary human fetal foreskin fibroblasts (HFFFs) with HCMV strain Merlin and initially used 8-plex TMT to quantify changes in PM protein expression. We assessed in biological duplicate three of the reference time points in productive HCMV infection and mock infection (experiment "PM1", Figure 1A). We quantified 927 PM proteins (Figure S1A available online). Surprisingly, 56% of proteins changed >2-fold and 33% >3-fold by 72 hr of infection. Replicates clustered tightly (Figure 1B).

We previously demonstrated that HCMV protein UL138 degrades the cell-surface ABC transporter Multidrug Resistance-associated Protein-1 (ABCC1) in both productive and latent infections and showed that the ABCC1-specific cytotoxic substrate Vincristine could be used therapeutically to eliminate cells latently infected with HCMV (Weekes et al., 2013). To validate findings in this present study of productive infection, we examined all quantified ABC transporters and found selective downregulation of ABCC1 as well as ABCC3 (Figure 1C). The ABCC3 drug transporter might represent an additional therapeutic target.

We further validated our results by comparison to all PM proteins that exhibit reported changes during productive HCMV infection in fibroblasts. We observed expected changes in 21/22 cellular proteins (Table S1A; Figure S1B) and detected six of six previously reported HCMV proteins at the PM. Five of these are virion envelope glycoproteins expressed late in infection (Figure 1D).

Temporal analysis of whole-cell lysates (WCLs) of HCMV-infected HFFFs enables the study of changes in expression of all proteins during infection and a comparison of the total abundance of a given protein to its expression at the PM. By analyzing WCL of HFFF infected simultaneously with PM samples, we again saw a high degree of reproducibility among biological replicates (experiment WCL1, Figures 1E and S1C) and confirmed changes in 31/35 previously reported proteins (Table S1B). We further validated our findings by comparison to a high-throughput western blot analysis of cells infected with Toledo strain of HCMV (Stanton et al., 2007) and saw a strong association between protein changes in both experiments ($p < 0.0001$, Fisher's exact test, Table S1C).

QTV to Screen for Antiviral Factors and Interferon-Induced Genes

To gain a more detailed view of changes in the host cell proteome and HCMV virome over the course of a productive infection, and to focus on events early in infection such as the IFN response, we used 10-plex TMT (McAlister et al., 2012). We analyzed productively infected HFFFs at seven time points, plus a duplicate mock infection (Figure S1D). For the tenth sample, we analyzed 12 hr infection with irradiated virus, in which viral DNA is inactivated, allowing for infection but preventing viral gene expression (Sullivan et al., 1971). Comparison of early productive infection and infection with irradiated virus allowed us to dissect the contribution of the virion to changes in the cellular proteome.

We quantified 1,184 PM proteins (experiment PM2, Figure S1E) and 7,491 cellular proteins (experiment WCL2, Figure 2A). Protein temporal profiles correlated well between repeat time courses (Figures 1F and S1F). Data from all four experiments are shown in Table S2, where the worksheet "Plots" is interactive, enabling generation of overlayed temporal graphs of PM and WCL expression of any of the human and viral proteins quantified.

Antiviral IFN effects are conferred by interferon-stimulated gene (ISG) products that target different stages of virus replication and include known herpesvirus restriction factors Viperin and IFI16 (Gariano et al., 2012). HCMV infection triggers expression of ISG, which the virus counters by impairing the IFN signaling pathway, degrading the double-stranded RNA sensor RIG-I (Retinoic acid-inducible gene I) and "repurposing" ISGs such as Tetherin to enhance rather than restrict viral replication (reviewed in Amsler et al., 2013). The temporal effects of these strategies on ISG protein expression are poorly understood as are the HCMV proteins responsible, although the immediate early proteins IE1 and IE2 and the apoptosis inhibitory protein vMIA have been implicated (Amsler et al., 2013).

One cluster of 40 proteins from experiment WCL2 (cluster A) exhibited striking upregulation at 6 and 12 hr after infection, followed by rapid return to near-basal levels (Figures 2A and 2B). Fourteen were viral proteins, and 26/40 were human, of which 85% are already known to be interferon responsive. Seventy-three percent of these proteins are additionally known to have antiviral function (Table S3A).

We therefore performed a comprehensive search of all other known interferon-induced antiviral genes, to determine which might be similarly or otherwise modulated during HCMV infection (Duggal and Emerman, 2012; Schoggins et al., 2011). Our results were consistent with the reported degradation of RIG-I and of the nuclear HCMV restriction factor Sp100 during infection (Figures 2A and S2A, respectively) (Kim et al., 2011a; Scott, 2009). Many of the tripartite motif-containing proteins (TRIMs) are interferon induced. TRIM5α can restrict HIV, although no viral factor is yet known to antagonize its expression (Rahm and Telenti, 2012). We quantified 21 TRIMs, of which TRIM 5, 16, 22, and 38 were downregulated during infection (Figure S2B). SAM Domain and HD Domain 1 (SAMHD1), zinc finger CCCH-type, antiviral 1 (ZAP/ZC3HAV1), and the novel anti-HIV factor Schlafen 11 (SLFN11) behaved similarly to members of cluster A (Figure S2A). It remains to be determined whether any of these antiviral proteins can restrict HCMV, and if reduction in their expression simply reflects diminished IFN signaling and response, or selective targeting by virus.

The relative contribution to ISG expression of active HCMV transcription (sensed, for example, by RIG-I) and viral binding to pattern recognition receptors (such as Toll-like receptor 2) is poorly understood (Paludan et al., 2011). We identified a group of 84 proteins significantly upregulated during productive infection, of which only 20% were >2-fold upregulated by irradiated virus (Figure 2C; Table S3B). The 84 proteins include 25/26 human proteins from cluster A, and 39% are known to be upregulated by IFN. Transcriptionally active HCMV may thus play an important role in ISG induction.

QTV Identifies Down- or Upregulated Signaling Pathways

The activity of a signaling pathway can be modulated either by posttranslational modification, or regulation of expression of a pathway member. Changes in protein expression can be quantified by QTV. We have shown that after an initial activation, the expression of ISG is rapidly reduced during HCMV infection, but how is this achieved? We quantified 13/15 key members of IFN induction and signaling pathways (Figure 3A, reviewed in

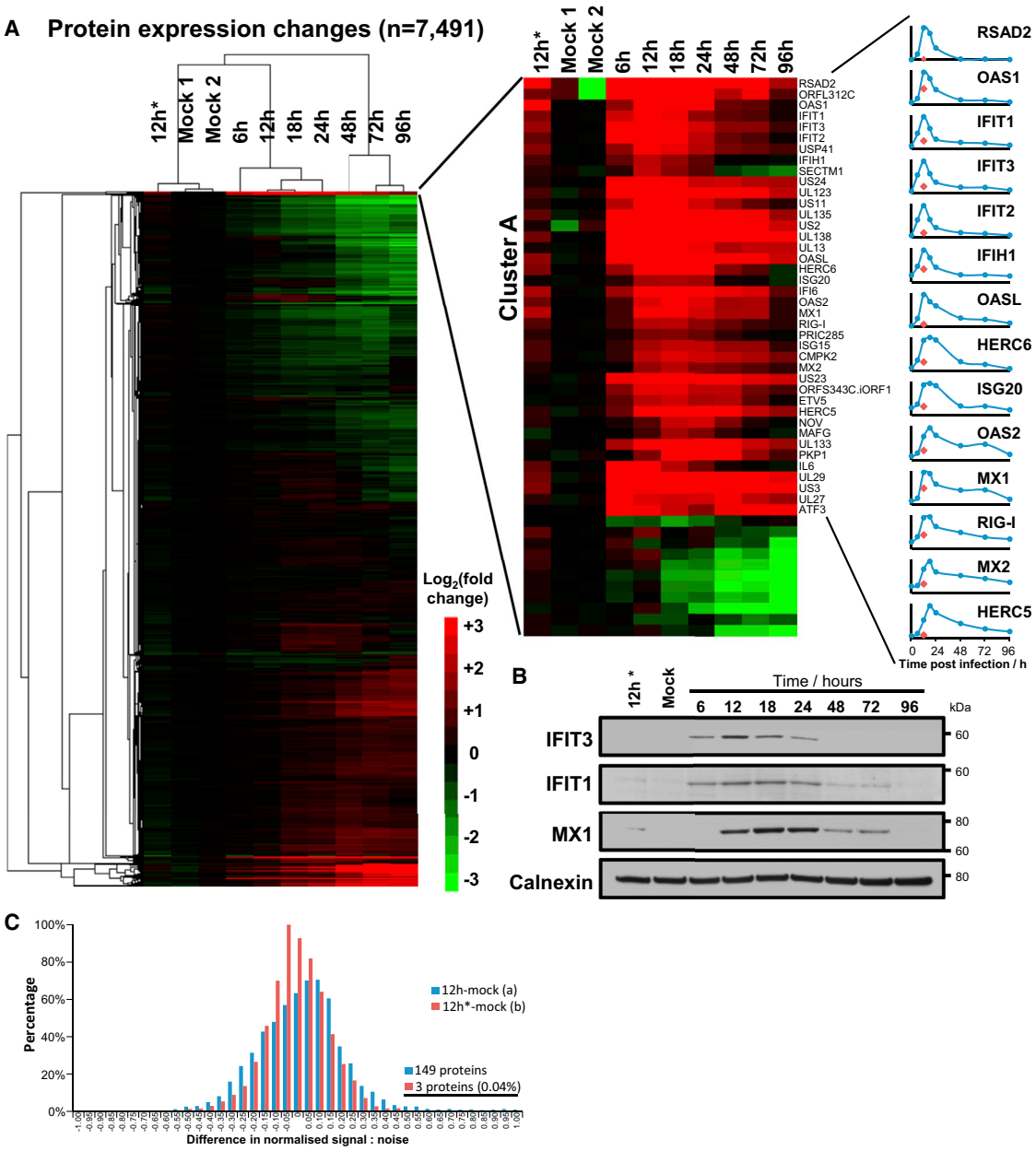

Figure 2. Temporal WCL Analysis of HCMV-Infected Fibroblasts Demonstrates Exquisite Regulation of ISGs

(A) Hierarchical cluster analysis of all proteins quantified in experiment WCL2, and enlargement of the top cluster A that included multiple IFN-induced antiviral proteins. Right panels, example temporal profiles. The y axis shows relative abundance of each protein. Red diamonds, 12 hr after infection with irradiated HCMV.

(B) Immunoblots of HFFF infected with HCMV confirm proteomic profiles.

(C) Interferon-induced proteins were more potently upregulated by productive infection than infection with irradiated HCMV. For each protein, signal:noise from the 12 hr irradiated virus or productive infection samples, and both mock samples was normalized to 1. The order of samples mock 1 and mock 2 was randomized into mock (a) and mock (b). The difference in normalized signal:noise was then calculated as indicated, and histograms were plotted. Where <0.05% of proteins were upregulated by infection with irradiated virus, 2% of proteins were upregulated by infection with live virus. These included 69 viral proteins and 84 human proteins, of which 39% are known ISGs.

See also Figure S2 and Table S3.

Amsler et al., 2013). We confirmed known effects of HCMV infection on Jak1, STAT2, and IRF9 (Le et al., 2008) and demonstrated that, apart from STAT1, expression of the final effectors in both interferon induction and response pathways were all progressively diminished during infection (Figure 3A). An effect of HCMV infection on IRF3 has not previously been reported.

The k-means method is useful to cluster proteins into a specified number of classes based on the similarity of temporal

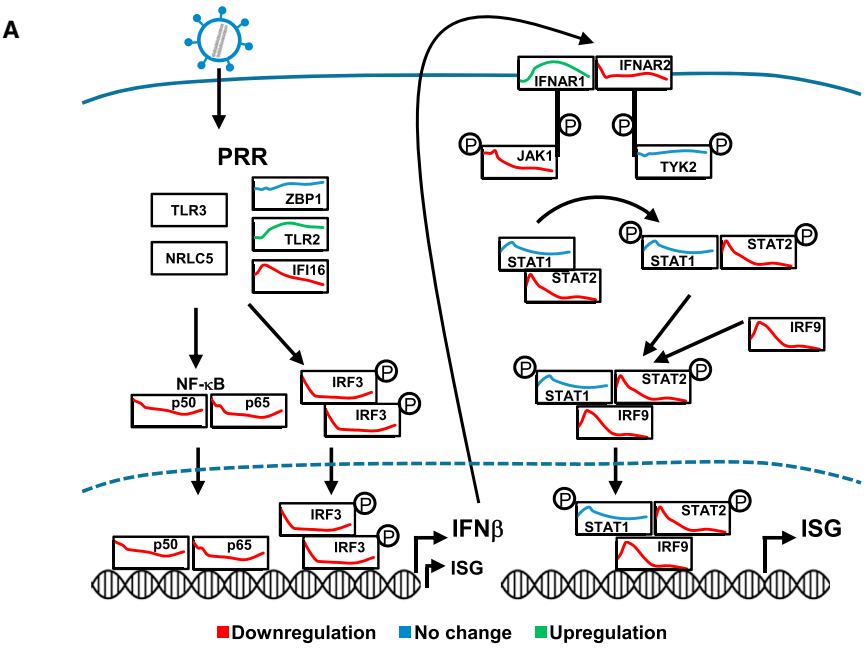

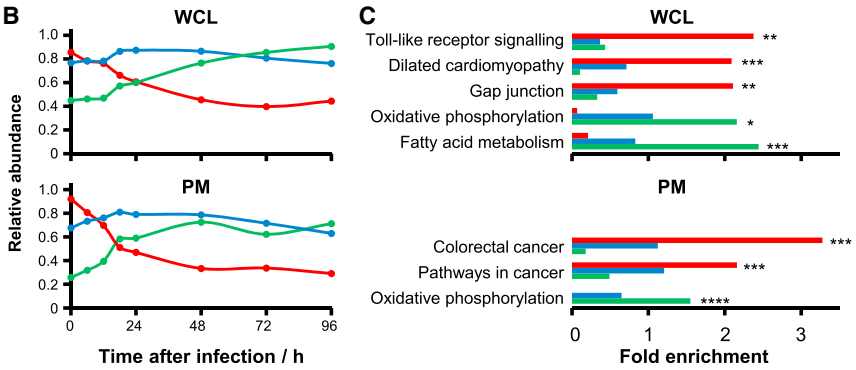

Figure 3. Modulation of Intracellular Signaling Pathways during HCMV Infection

(A) Quantitation of interferon induction and response pathways. The temporal profile of each protein is shown over 96 hr of infection, and colored red (downregulation), blue (unchanged), or green (upregulation). Data were derived from experiment WCL2 apart from IFNAR1 and IFNAR2, from PM2. Expression of certain ISGs is known to occur in the absence of IFN, in an IRF3-dependent manner. PRR, pattern recognition receptors.

(B) Average temporal profiles from 3-class k-means clustering of proteins quantified in experiments WCL2 and PM2. The three classes divided proteins into downregulated (red), unchanged (blue), or upregulated (green).

(C) Enrichment of KEGG pathways within each class was determined using DAVID software, against a background of all quantified proteins. Benjamini-Hochberg adjusted p values are shown for each indicated bar (*$p < 0.00001$, **$p < 0.0001$, ***$p < 0.01$, ****$p < 0.05$). Individual pathways are shown in Figures S3A–S3C, and pathway members are shown in Table S4.

profiles. We clustered all 7,491 proteins from experiment WCL2 and 1,184 proteins from PM2 into three classes (corresponding to upregulation, downregulation, and no change) to identify novel pathways dysregulated during HCMV infection (Figure 3B). We then applied DAVID software (Huang et al., 2009) to determine which KEGG (Kyoto Encyclopedia of Genes and Genomes) pathways were enriched in each class (Figures 3C and S3A). We made the discovery that multiple members of the TLR signaling pathway were downregulated (Figures S3A and S3B; Table S4A), suggesting that HCMV might employ a number of strategies to avoid this intrinsic immune mechanism. Fatty acid metabolism and oxidative phosphorylation were upregulated during infection (Figure 3C; Table S4A), corresponding to published literature (Koyuncu et al., 2013).

A lack of gap junction intercellular communication is common in cancer, and is thought to enable escape of homeostatic control. Gap junction alpha-1 protein (GJA1) modulates the expression of many genes involved in cell-cycle control and tumorigenesis and is degraded by HCMV IE1 and IE2 (Khan et al., 2014; Stanton et al., 2007). We confirmed GJA1 downregulation and found multiple other members of the gap junction signaling pathway similarly changed (Figure S3B; Table S4A).

The KEGG pathways "colorectal cancer" and "pathways in cancer" were enriched in the downregulated PM cluster and included Frizzled receptors FZD1, 2, 4, 6, and 7 and signaling protein WNT5a, all key members of the wnt pathway. We additionally discovered downregulation of the canonical wnt pathway coreceptors LRP5 and 6, and of noncanonical receptors ROR1, ROR2, RYK, and PTK7. Overall, 11/13 quantified wnt receptors were downmodulated (Figure S3D). Diminished transcription of wnt target genes and increased degradation of the key wnt mediator β-catenin have been reported in HCMV infection; however, the underlying mechanism is unclear (Angelova et al., 2012). Our discovery of downregulation of the majority of all wnt receptors suggests that diminished basal signaling from the cell surface may lead to increased proteasomal β-catenin degradation. Multiple effects on different cell-surface receptors suggest that the modulation of this signaling pathway may be of paramount importance to HCMV.

In order to expand our search, we performed gene set enrichment analysis (GSEA) based on the average k-means profiles for up-and downregulated WCL clusters (Figure 3B) (Subramanian et al., 2005). GSEA can increase the power to detect enrichment because it scores pathways based on similarity of protein members to a prototypic profile, as opposed to determining enrichment within a large group of proteins with broadly similar profiles. Multiple mitochondrial metabolic and biosynthetic pathways were significantly upregulated and confirmed the changes

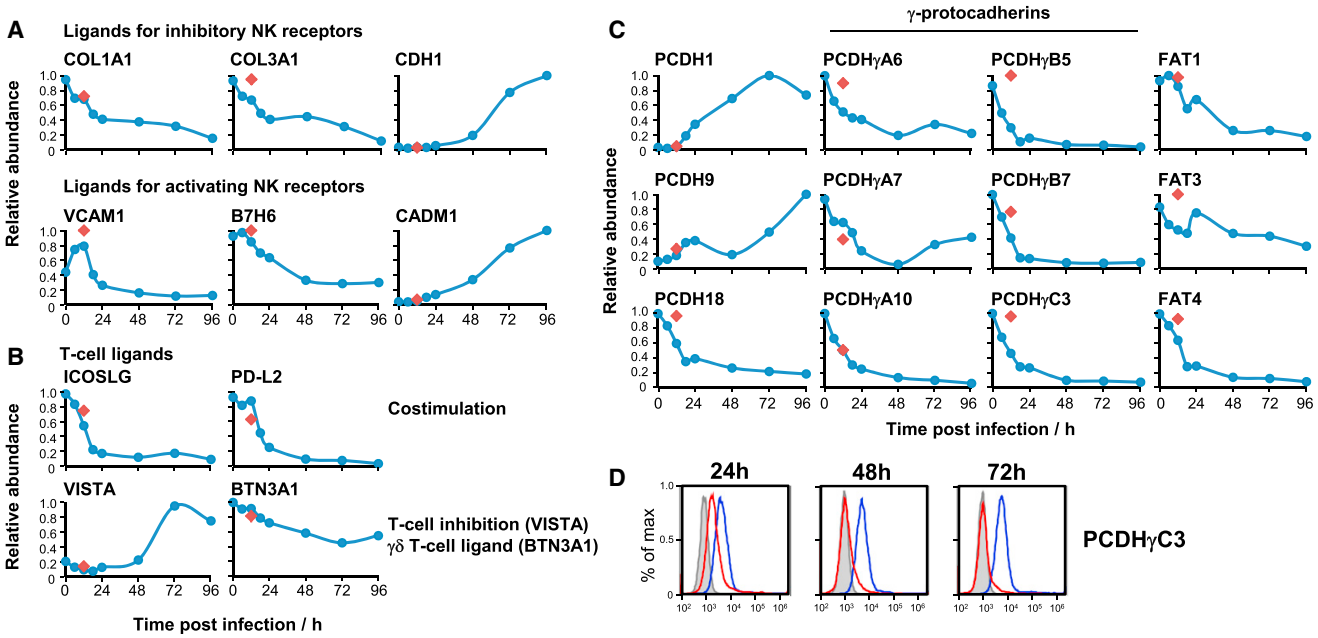

Figure 4. Temporal Changes in Known and Putative Cell-Surface Immunomodulators

(A) Temporal profiles of known NK ligands whose modulation by HCMV had not previously been recognized.

(B) Temporal profiles of T cell ligands not previously known to be modulated during infection.

(C) Temporal profiles of all quantified protocadherins.

(D) Validation of the temporal profile of PDCHγC3 by flow cytometry.

Red diamonds, 12 hr after infection with irradiated HCMV. See also Figure S4, Table S5, and Data S1.

we observed in fatty acid metabolism and oxidative phosphorylation. Transcription and export of mRNA was upregulated. Downregulated pathways included Robo receptor signaling, important in cell proliferation and motility, and ERBB and VEGFR signaling (Table S4B).

Discovery of NK and T Cell Ligands and Families of Other Cell-Surface Receptors/Ligands Modulated by HCMV Infection

We mined our data for all known NK cell ligands (Vivier et al., 2008) and discovered previously unrecognized modulation of six ligands during HCMV infection. E-cadherin (CDH1), the ligand for the inhibitory NK receptor KLRG-1 (killer cell lectin-like receptor subfamily G member 1), was dramatically upregulated during infection. Vascular cell adhesion molecule 1 (VCAM1) and B7-H6, ligands for activating NK receptors α4β1 integrin and NKp30, were downregulated (Figure 4A). Interestingly, other known ligands including collagen I (COL1A1 and COL1A2), collagen III (COL3A1), cell adhesion molecule-1 (CADM1), and poliovirus receptor-related 1 (PVRL1) were expressed in a manner that would be expected for an appropriate response to intracellular infection (Figure 4A; Table S2).

We performed a similar screen for all known αβ T cell costimulatory molecules, and γδ T cell ligands (Bonneville et al., 2010; Hubo et al., 2013). The T cell costimulators ICOSLG (inducible T cell costimulator ligand) and PD-L2 were downregulated during infection, as was butyrophilin subfamily 3 member A1 (BTN3A1), recently shown to present phosphoantigens to Vγ9Vδ2$^+$ T cells (Vavassori et al., 2013). V-domain Ig suppressor of T cell activation (VISTA, C10Orf54), a novel B7 family inhibitory ligand (Ceeraz et al., 2013) was upregulated late in infection (Figure 4B).

NK and T cell ligands belong to a few key protein families, including cadherins, C-type lectins, immunoglobulin, TNF receptor, and major histocompatibility-complex-related molecules (Vivier et al., 2008). In order to discover immunomodulating proteins, we added InterPro functional domain annotations to data from experiments PM1 and PM2 (Hunter et al., 2012) and reasoned that modulation of a ligand during HCMV infection may indicate biological importance. Seventy-four proteins had a relevant InterPro annotation and at least a 4-fold change compared to mock infection (Table S5A; Data S1). Eight downregulated proteins were protocadherins. Examining all quantified proteins in this family, we found that six of six γ-protocadherins were particularly potently downregulated (Figure 4C). The protocadherins may therefore represent a major set of immunomodulators.

We confirmed temporal profiles of protocadherins PCDHγC3 and FAT1 in addition to eight other cell-surface proteins by flow cytometry and immunoblot (Figures 4D and S4A, S4C, and S4E). To provide proof-of-principle validation of our functional predictions, we performed siRNA-mediated knockdown of the C-type lectin CLEC1A (Table S5A), which is downregulated 7-fold by HCMV and is a potential NK ligand by homology to CLEC2D. Polyclonal NK-cells from three of three independent donors demonstrated reduced degranulation to autologous

targets upon knockdown of CLEC1A suggesting that this molecule may be a novel activating NK ligand (Figure S4D). We observed similar results for the protocadherin FAT1, providing initial confirmatory evidence that members of this family may indeed be involved in immunoregulation (Figure S4E). CEACAM-1 (immunoglobulin family) was upregulated 20-fold by HCMV infection and may have roles in T cell regulation. Using a blocking antibody, we demonstrated increased degranulation of $CD8^+$ T cells specific for an HCMV HLA-A2 restricted peptide epitope suggesting that upregulation of this molecule in infected cells may inhibit cytotoxic T cell-mediated lysis (Figure S4F).

There is increasing evidence for a substantial role of plexin-semaphorin signaling in the immune system (Takamatsu and Kumanogoh, 2012). For example, secreted class III semapohrins bind plexins A and D1 to regulate migration of dendritic cells to secondary lymphoid organs. Plexin B2 interacts with membrane-bound semaphorin 4D to promote epidermal $\gamma\delta$ T cell activation (Witherden et al., 2012). HCMV infection substantially downregulated five of the nine plexins: A1, A3, B1, B2, and D1. Intriguingly, neuropilin 2, a plexin coreceptor was also rapidly downregulated. Semaphorin 4D was dramatically upregulated and 4C downregulated, suggesting that viral interaction with these ligands is complex (Table S5A; Data S1).

To determine which protein domains and biological processes were enriched within highly downregulated PM proteins, we used DAVID software (Huang et al., 2009). The Interpro categories ''protocadherin gamma'' and ''immunoglobulin-like fold'' were significantly enriched in addition to Gene Ontology (GO) biological processes ''regulation of leukocyte activation'' and ''positive regulation of cell motion,'' suggesting a negative effect of HCMV on cell motility. DAVID analysis also revealed families of downregulated proteins, including six G-protein-coupled receptors from the rhodopsin-like superfamily (Table S5B).

Within the category ''regulation of leukocyte activation,'' ephrin B1 was downregulated, and we therefore examined all ephrins and their receptors. We observed striking downregulation of ephrins B1 and B2 as well as all three of their quantified B-class ephrin receptors (Data S1). Downstream effects of forward or reverse ephrin signaling include changes in cell adhesion, shape, and motility, and there is evidence for a role of ephrin B2 in murine T cell costimulation (Nikolov et al., 2013), suggesting that downregulation of this pathway may represent another mechanism of immune evasion.

Temporal Analysis of HCMV Viral Protein Expression

Most prior studies of the temporal expression of canonical HCMV proteins have employed immunoblots at only one or a few time points. Comparison between different reports has been complicated by lack of specific antibodies and study-to-study variation in the HCMV strain used, with laboratory-adapted strains AD169 and Towne (which lack a large number of ORFs as a result of extensive passage in vitro) often used in preference to isolates containing a complete genome (Ma et al., 2012). We were able to quantify the temporal expression of the majority (139/171) of the canonical HCMV proteins as well as 14 non-canonical ORFs; most of these proteins were quantified in a single experiment (Figure 5, plots for all quantified viral proteins in Data S1).

IE/E/E-L/L cascades are functionally defined by the use of metabolic inhibitors. IE transcripts accumulate in the presence of a protein synthesis inhibitor such as cycloheximide. Expression of early genes is unaffected by viral DNA synthesis inhibitors such as Phosphonoformate (PFA), whereas E-L genes are partially inhibited, and L genes completely inhibited (Chambers et al., 1999).

A complementary method of classification would be to group viral proteins according to their temporal profiles. Use of the k-means method with four classes suggested that HCMV protein profiles grouped similarly to the recognized functional cascades IE/E/E-L/L (Figure 5A). We performed k-means clustering with 2 to 14 classes and assessed the summed distance of each protein from its cluster centroid. Although this summed distance necessarily becomes smaller as more clusters are added, the rate of decline decreases with each added group, eventually settling at a fairly constant rate of decline that reflects overfitting; clusters added prior to this point reflect underlying structure in the temporal protein data, whereas clusters subsequently added through overfitting are not informative. The point of inflexion fell between five and seven classes, suggesting that there are at least five distinct temporal protein (Tp) profiles of viral protein expression (Figures 5A–5D). We term these classes Tp1, Tp2, Tp3, Tp4, and Tp5. There was generally good correspondence between classical functional and protein temporal classes, for example, the known L proteins UL99, UL94, UL75, UL115, and UL32 all classified as Tp5 (Omoto and Mocarski, 2014). A cluster of 13 proteins that we call Tp4 exhibited a distinct profile to Tp3 and Tp5, with maximal expression at 48 hr and low expression at other time points (Figures 5C and 5D). Members of this cluster predominantly originated from two regions of the viral genome (Table S6A).

To directly compare classical functional and protein temporal classes, we performed WCL analysis in the presence or absence of the viral DNA replication inhibitor PFA (experiment WCL3, Figures 5C and 5D; Table S2; plots for all quantified viral proteins in Data S1). Expression of 48/55 Tp5-class proteins was completely or almost completely inhibited by PFA. Tp3 and Tp4 proteins were generally partially inhibited, with little effect on Tp1 or Tp2. Some proteins displayed more complex profiles, with enhanced expression later in infection with PFA block (Data S1).

Eight proteins appear earlier in infection than had previously been understood. UL27, UL29, UL135, UL138, US2, US11, US23, and US24 all exhibited peak expression at 6–18 hr after infection (Figure 5C). UL29 and US24 appeared particularly early, with peak expression at only 6 hr postinfection, which may correspond with their suggested ability to stimulate IE gene expression (Feng et al., 2006; Terhune et al., 2010).

We were unable to confidently resolve the profile of UL122 (IE2). UL122 and UL123 are expressed by alternative splicing of a single major immediate-early transcript. Exons 1, 2, 3, and 4 encode UL123 and exons 1, 2, 3, and 5 encode UL122; however, additional transcripts have also been detected from the region of exon 5 (Stenberg et al., 1989; Stern-Ginossar et al., 2012). We examined each peptide quantified from every exon (Figure S5A). The profiles of all peptides from exon 4 peaked at 18–24 hr, corresponding to the predicted expression of UL123

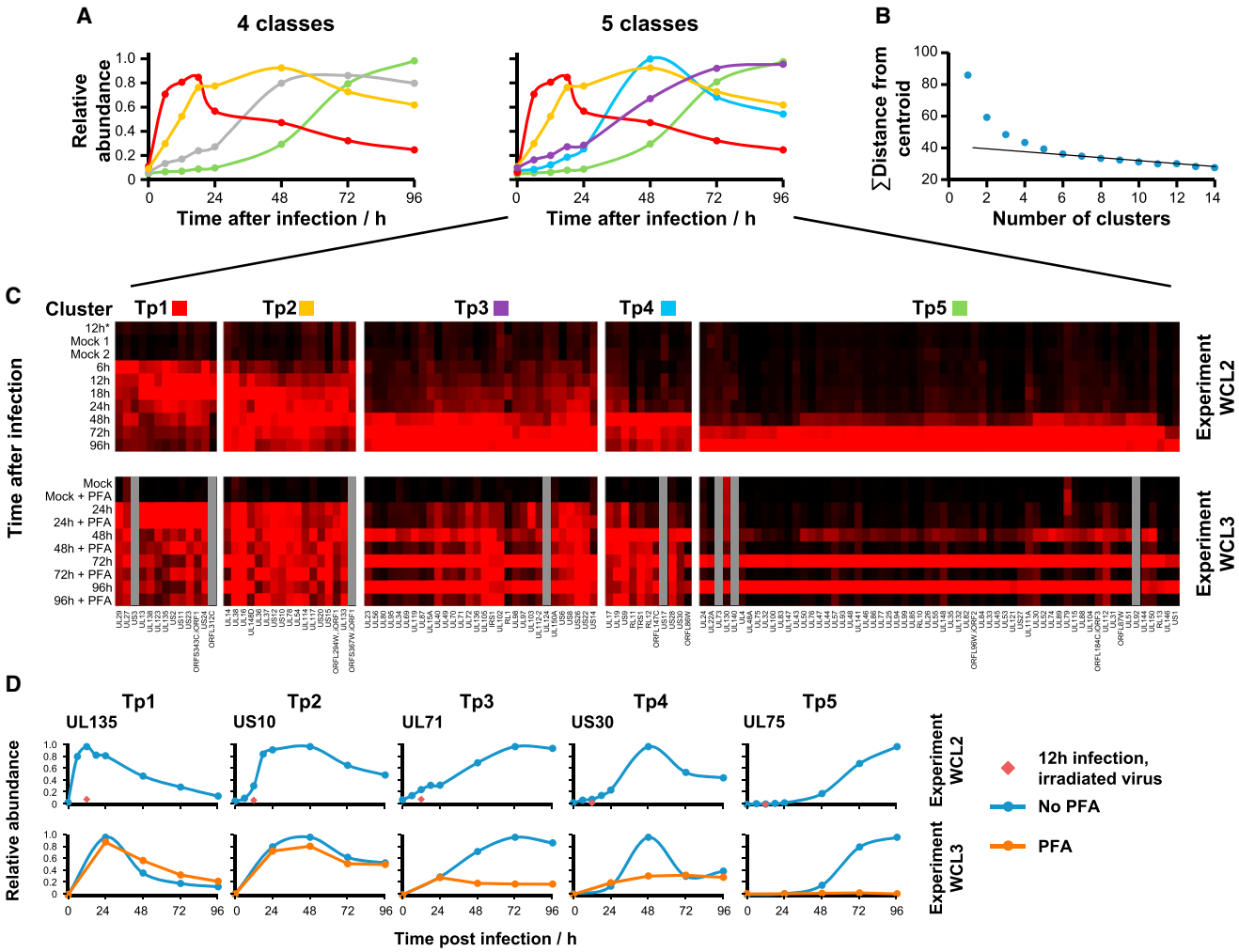

Figure 5. Definition of Temporal Classes of HCMV Gene Expression

(A) The k-means method was used to cluster all quantified HCMV proteins (experiment WCL2) into four or five classes. Shown are the average temporal profiles of each class. With four classes, proteins grouped into classes similar to the classical IE/E/E-L/L cascades. With five classes, a distinct temporal profile appeared (blue).

(B) Number of temporal classes of HCMV gene expression. The summed distance of each protein from its cluster centroid was calculated for one to 14 classes and plotted. The point of inflexion fell between five and seven classes.

(C) Top: temporal profiles of proteins in each k-means class (experiment WCL2) were subjected to hierarchical clustering by Euclidian distance. Both UL112 and isoform p50 of UL112 (UL112-2) were quantified. UL122 was excluded from clustering due to uncertainty in peptide assignment. Bottom: experiment WCL3. Viral protein profiles were further assessed in the presence or absence of the viral DNA replication inhibitor PFA. Proteins are displayed in the same order as the clusters defined in the upper panels.

(D) Temporal profiles of typical proteins from each cluster (upper panel), and the corresponding profiles in the presence or absence of PFA (lower panel).

See also Figure S5, Table S6, and Data S1.

protein. The profiles of ten exon 5 peptides corresponding to the late-expressed internal ORF, ORFL265C.iORF1 (Stern-Ginossar et al., 2012) peaked at 96 hr. A single peptide N-terminal to this ORF that is likely to originate from UL122 had a distinct profile with expression from 6 hr that peaked at 48 hr, similar to UL122 mRNA (Stern-Ginossar et al., 2012). This suggests the existence of at least two proteins arising wholly or in part from exon 5 and corresponds to the detection of an abundant late 40 kDa protein, previously detected from the same internal exon 5 ORF of AD169 strain (Stenberg et al., 1989). It is likely that ORFL265C.iORF1 protein is more abundant than UL122, effectively masking the earlier signal from most UL122 exon 5 peptides. Our quantitation of DNA polymerase processivity subunit UL44 may similarly have been complicated due to multiple transcription start sites (Data S1).

We further compared our protein-level data with recent RNA-sequencing-based temporal analysis of HCMV Merlin strain transcripts at 5, 24, and 72 hr postinfection in HFFF (Stern-Ginossar et al., 2012). We again used 5 k-means classes to group transcripts based on their temporal profiles (Figure S5C).

Because there were no intermediate mRNA time points between 5 and 24 hr, or between 24 and 72 hr, there was insufficient information to make an accurate comparison between the central three mRNA clusters and our Tp2, Tp3, or Tp4 class proteins. We therefore used mRNA data to define three classes: Tr1, Tr2–4, and Tr5 (Figure S5C). Comparison to our protein data was striking: 10/13 Tp1 proteins were also Tr1 transcripts and 49/55 Tp5 proteins were Tr5 transcripts ($p < 0.0001$, Fisher's exact test) (Table S6C; Figure S5D). Such correspondence between different studies targeting distinct classes of biomolecules suggests that the temporal classes of HCMV gene expression we define are likely to be biologically relevant.

We quantified the full temporal profiles of nine noncanonical HCMV ORFs. Four ORFs related to canonical HCMV proteins (N-terminal extension, internal ORF, C-terminal extension) and demonstrated similar temporal profiles to their canonical counterparts (Figure S5B; Data S1). Five ORFs were encoded either in different reading frames, or on the reverse strand to canonical genes (Table S6B). We additionally quantified five further noncanonical ORFs in experiment WCL3 (Data S1).

HCMV Proteins Present at the Cell Surface

Viral proteins present at the surface of an infected cell may be therapeutic antibody targets. To date, only six HCMV proteins have been demonstrated at the PM of infected fibroblasts, all late in infection, which we have confirmed (Figure 1D). Several other studies transduced individual viral genes and demonstrated protein appearance at the cell surface, which can indicate but may not reflect protein location during productive infection (Table S7).

We detected a total of 67 viral proteins in experiments PM1 and PM2. Plasma membrane profiling provides a very substantial enrichment for PM glycoproteins (up to 90% of proteins from unfractionated samples, and approximately 60% of proteins from fractionated samples have indicative Gene Ontology (GO) terms (Figure S1A) (Weekes et al., 2012). Subcellular localization of viral proteins is, however, poorly annotated, making it difficult to determine which might be non-PM contaminants, such as abundant viral tegument and nuclear proteins. We therefore developed a filtering strategy: for every GO-annotated human protein quantified in experiment PM1 or PM2 (Figure S1A), we calculated the ratio of peptides (experiments PM1 + PM2)/(experiments WCL1+WCL2). Ninety-two percent of proteins that were GO-defined non-PM had a ratio of <1.4; 88% of human proteins scoring above 1.4 were annotated as PM proteins, demonstrating the predictive value of this metric (Figure 6A). Applying this filter, we defined 29 high-confidence viral PM proteins, which included the majority of viral proteins previously identified at the surface of either infected or transduced cells, and excluded all proteins unlikely to be present at the cell surface based on their known function (Table S7).

In general, we observed a striking correlation between the PM2 and WCL2 temporal profiles of all 29 high-confidence proteins. For the subset of known virion envelope glycoproteins (Varnum et al., 2004), protein expression at the PM was significantly later than in WCL, confirmed by analysis of the same proteins from experiments PM1 and WCL1 (Figures 6B and S6). This may reflect assembly of the HCMV virion within the viral cytoplasmic assembly compartment prior to viral egress (Alwine, 2012) and demonstrates that QTV can additionally provide insights into aspects of the viral life cycle. PM appearance of UL119 was similarly delayed, suggesting that this known virion glycoprotein may be a component of the virion envelope. The sensitivity of MS3 TMT-based mass spectrometry is suggested by our apparent quantitation of binding or fusion of viral envelope with the plasma membrane; there was a small early peak in PM presence of most virion envelope glycoproteins at 6 hr of infection that disappeared by 12 hr (Figure 6B).

QTV Indicates Mechanism of Action of Viral Proteins

We have previously shown that HCMV UL141 retains the poliovirus receptor (PVR) in the endoplasmic reticulum, inhibiting cell-surface expression and preventing interaction with activating NK receptor DNAM-1. Intracellular PVR accumulates during HCMV infection. In contrast, a second DNAM-1 ligand poliovirus receptor-related 2 (PVRL2) is targeted for proteasomal degradation by UL141 acting with other HCMV gene(s) (Prod'homme et al., 2010; Tomasec et al., 2005). QTV confirmed these results; we observed rapid depletion of PVR from the plasma membrane, in contrast to its accumulation within WCL. PVRL2 was lost from both PM and WCLs (Figure 7). The WCL kinetics of UL141 expression paralleled that of PVR but were inversely related to PVRL2.

The activating receptor NKG2D is expressed on a variety of immune effector cells and recognizes major histocompatibility complex class I-related ligands MICA, MICB, and ULBP1-3. HCMV infection strongly induces transcription of MICB, ULBP1, and ULBP2 mRNA but prevents their surface expression by intracellular sequestration with HCMV UL16 (Dunn et al., 2003a). Our data were highly consistent with this literature. Interestingly, cell-surface expression of ULBP1 and -2 rose late in infection, suggesting that UL16 had become overwhelmed (Figure 7A).

We therefore examined other HCMV proteins known to target cell-surface receptors (Table S1A). The profiles of UL138 and ABCC1 were consistent with their codegradation (Weekes et al., 2013), and the profile of HLA-A reflected US2 and US11-mediated degradation (Figure 7B). Other examples are shown in Figures S7A and S7B. The temporal profiles provided by QTV are thus useful to gain mechanistic insights into known interactions between viral and host proteins.

DISCUSSION

In this study, we provide a comprehensive resource describing temporal changes in viral and host proteomes during infection with HCMV. Simultaneous study of protein expression at the cell surface and in whole-cell lysates has revealed insights into many aspects of the viral life cycle. To be able to persist in an infected individual lifelong, herpesviruses have developed a wealth of strategies to modulate innate and adaptive immunity. One benefit is that we can use HCMV infection to discover proteins important in host defense, as viral modulation of protein expression generally reflects biological imperative. We often observed modulation of multiple members of the same protein family, increasing the likelihood of biological relevance; for

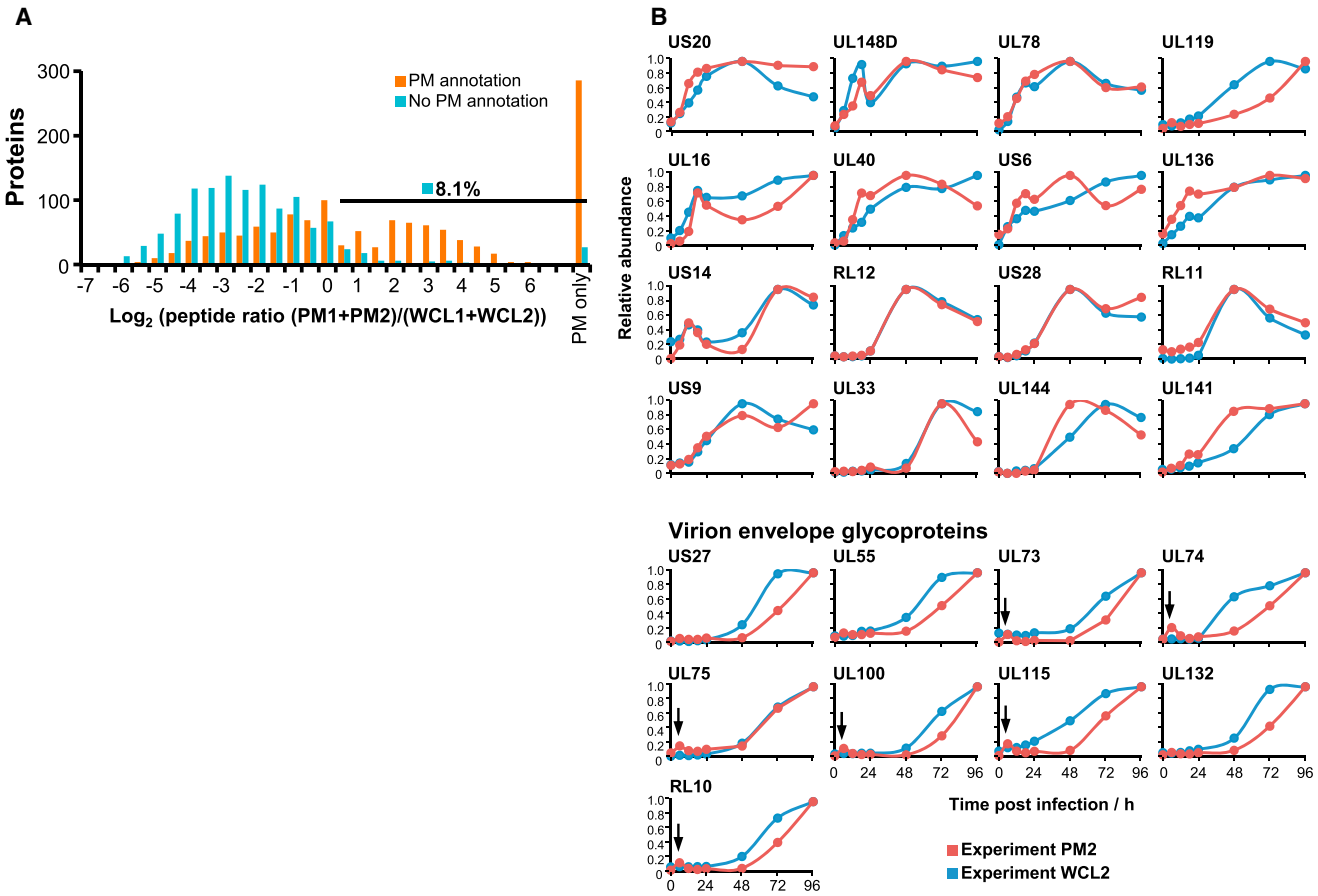

Figure 6. HCMV Proteins Quantified at the Surface of Infected Fibroblasts

(A) Histogram of peptide ratios for all GO-annotated proteins quantified in experiments PM1 or PM2. "PM only," not detected in experiments WCL1 or WCL2. "PM annotation": "plasma membrane", "cell surface," "extracellular," or "short GO."

(B) Temporal profiles of all high-confidence PM proteins (Table S6). Virion envelope glycoproteins were generally detected significantly earlier in whole-cell lysates than in plasma membrane samples. Arrows, quantitation of fusion or binding of the virion envelope and the plasma membrane.

See also Figure S6 and Table S7.

example, six of six γ-protocadherins that are downregulated during infection may be novel NK ligands in addition to protocadherin FAT1. The correspondence in temporal profiles of proteins in cluster A (Figure 2A) enables prediction of IFN-stimulated genes, which might additionally have antiviral function. Multiple signaling pathways were modulated by HCMV, which has the potential to inform not only viral interaction networks by predicting effects on pathway target genes but improves our knowledge of the metabolic changes necessary to effect viral replication (Koyuncu et al., 2013). GSEA provides a particularly useful overview of many of the pathways and receptors changing significantly in our data.

The temporal quantitation of >80% of canonical HCMV proteins in one experiment provides a significant technical advance. Our knowledge of HCMV protein profiles has so far relied on a literature complicated by the use of multiple different laboratory-adapted viral strains, different cell types, and variable infection conditions (Ma et al., 2012). Many have not previously been quantified. We provide a temporal system of classification of HCMV protein expression using the prototype clinical strain Merlin, which is complementary to and consistent with the functionally derived classical IE/E/E-L/L nomenclature. For example, expression of 87% of proteins we define as Tp5 was prevented by the viral DNA replication inhibitor PFA. These data suggest that the classical "true late" category of transcripts could be substantially expanded. Furthermore, all capsid proteins we quantified (Mocarski et al., 2013) belonged to class Tp5, whereas viral tegument proteins were more diverse: of 27 quantified, three were Tp1, 2 Tp2, 8 Tp3, and 14 Tp5, suggesting that these proteins may additionally have nonstructural roles such as regulation of gene expression and immune evasion. It remains to be seen whether Tp4 proteins have a distinct function that requires peak expression at 48 hr of infection, for example, preparation of the cell for virus release via inhibition of neutralizing antibody and cellular immunity (RL11 family), or promoting viral egress and cell-cell spread (Table S5A). Particular advantages to our temporal measurements include the ability to correlate viral and cellular protein expression, narrowing the field of viral proteins possibly

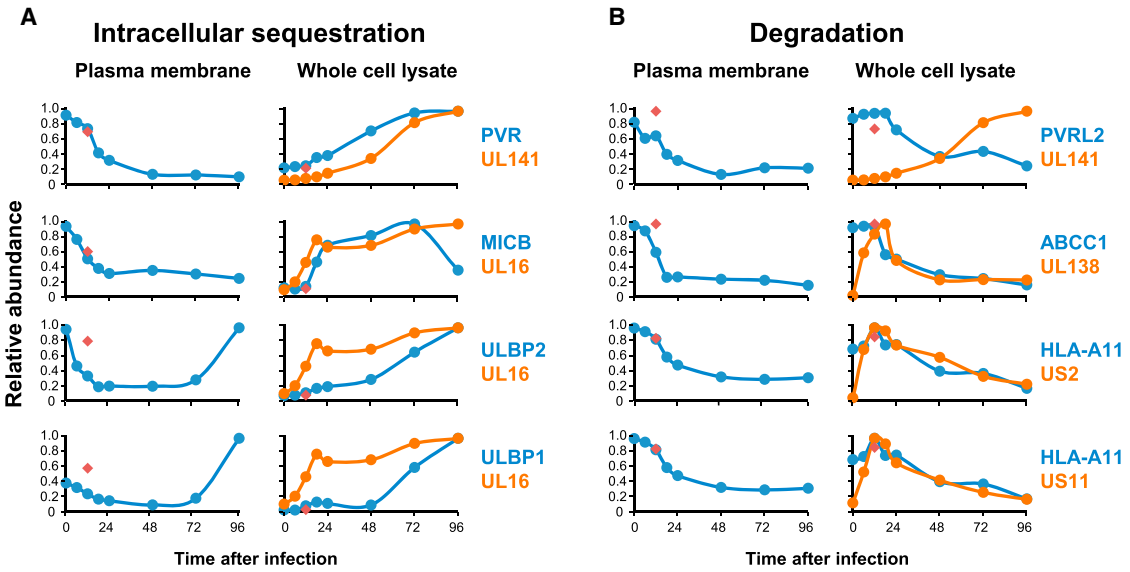

Figure 7. QTV Provides Mechanistic Insights into Downregulated Cell-Surface Targets

(A) Proteins that are known to be sequestered within the cell accumulated in WCL samples during infection.

(B) Proteins targeted for lysosomal or proteasomal degradation declined during infection.

Red diamonds, 12 hr after infection with irradiated HCMV. See also Figures S7A and S7B.

responsible for target modulation and in some cases indicating mechanism. The utility of QTV could be extended by simultaneous transcriptomic studies; if a host protein is downregulated, is this due to diminished gene expression, or posttranscriptional effects such as protein degradation?

In their recent ribosomal profiling (RP) analysis of HCMV, Stern-Ginossar et al. (2012) identified 147/171 canonical genes. We quantified 139/171 proteins (Table S2), notably including 15 genes not detected by RP. Proteins UL1 and UL6 were quantified at the PM but not in WCL samples suggesting that overall abundance of both mRNA and protein might be low. It is unclear why RP failed to detect the 13 remaining proteins, which in several cases we quantified by abundant peptides. It is likely that the sensitivity of QTV for low-abundant proteins will be further increased with the next generation of Orbitrap mass spectrometers, enabling an even more comprehensive coverage of both HCMV and human proteomes. For example, analysis of experiment WCL3 using the new Orbitrap Fusion enabled quantitation of five noncanonical ORFs we previously did not detect. Even with this sensitive instrument, it is still possible that we were unable to detect very low-abundant proteins, which may explain why some studies have detected viral transcripts earlier in infection that our protein measurements suggest. An increase in proteome coverage will also improve our ability to distinguish protein isoforms, which complicated our quantitation of UL122.

With an increasing frequency of transplantation and emergence of drug resistance, novel strategies are required to treat HCMV infection. QTV provides evidence for up to 29 cell-surface viral glycoproteins that can now be assessed as targets for therapeutic monoclonal or bispecific antibodies, to stimulate antibody-dependent cellular cytotoxicity or deliver a cytotoxin. Strongly upregulated PM proteins may constitute alternative antibody targets. By directing treatment toward proteins expressed early in infection, it may be possible to eliminate infected cells prior to the release of infectious virus. The efficacy and safety of such an approach is suggested by small-scale treatment of patients with severe drug-resistant HCMV disease using pooled immunoglobulin selected for high antibody titers to HCMV (Alexander et al., 2010). QTV has demonstrated great utility in being able to identify and quantify the regulation of virus and host proteins on the cell surface without requirement for specific antibodies. Clearly, the cell-surface viral proteins we describe require validation using an independent approach once reagents are available.

QTV is applicable to any virus, or indeed any intracellular pathogen with a robust in vitro model and has the potential to improve our understanding of infection.

EXPERIMENTAL PROCEDURES

Brief descriptions of key experimental procedures are provided below. For complete details, see Extended Experimental Procedures.

Virus Infections

Twenty-four hours prior to each infection, 1.5×10^7 HFFFs were plated in a 150 cm^2 flask. Cells were sequentially infected at multiplicity of infection 10 with HCMV strain Merlin. Greater than 95% of cells were routinely infected using this approach (Figures S4A and S4B). Infections were staggered such that all flasks were harvested simultaneously. For 12 hr irradiated virus infection, virus was gamma irradiated with a dose of 3,500 Gy.

Protein Isolation and Peptide Labeling with Tandem Mass Tags

Plasma membrane profiling was performed as described previously (Weekes et al., 2012). One hundred percent of each peptide sample was labeled with TMT reagent, and six fractions were generated from combined peptide samples by tip-based strong cation exchange. For whole-proteome analysis, cells

were lysed and protein was reduced and then alkylated. Protein was digested with LysC (experiment 1) or LysC and then Trypsin (experiments 2 and 3). Peptides were labeled with TMT reagent, and 12 fractions were generated by high-pH reverse-phase HPLC.

Mass Spectrometry and Data Analysis

We performed mass spectrometry using an Orbitrap Elite (experiments 1 and 2) or an Orbitrap Fusion (experiment WCL3) and quantified TMT reporter ions from the MS3 scan (McAlister et al., 2012; Ting et al., 2011). Peptides were identified and quantified using a Sequest-based in-house software pipeline. A combined database was searched, consisting of (1) human Uniprot, (2) Merlin strain HCMV Uniprot, and (3) all additional noncanonical HCMV ORFs (Stern-Ginossar et al., 2012). Peptide-spectral matches were filtered to a 1% false discovery rate (FDR) using linear discriminant analysis in conjunction with the target-decoy method (Huttlin et al., 2010). The resulting data set was further collapsed to a final protein-level FDR of 1%. Protein assembly was guided by principles of parsimony. Where all PSM from a given HCMV protein could be explained either by a canonical gene or noncanonical ORF, the canonical gene was picked in preference. Proteins were quantified by summing TMT reporter ion counts across all matching PSM after filtering based on isolation specificity (Pease et al., 2013). Reverse and contaminant proteins were removed, and protein quantitation values were exported for normalization and further analysis in Excel. Hierarchical clustering was performed using centroid linkage with Pearson correlation unless otherwise noted. One-way ANOVA was used to identify proteins differentially expressed over time in experiments PM1 and WCL1, and p values were corrected for multiple testing using the method of Benjamini-Hochberg. Other statistical analysis was performed using XLStat.

NK and T Cell CD107a Mobilization Assays

NK and T cell degranulation assays were performed in a similar manner to that described previously (Prod'homme et al., 2010). These protocols were approved by the Cardiff University School of Medicine Ethics Committee Ref. no: 10/20.

SUPPLEMENTAL INFORMATION

Supplemental Information includes Extended Experimental Procedures, seven figures, one data file, and seven tables and can be found with this article online at http://dx.doi.org/10.1016/j.cell.2014.04.028.

AUTHOR CONTRIBUTIONS

M.P.W. and P.T. designed the experiments and wrote the manuscript. M.P.W., P.T., C.A.F., R.J.S., E.C.Y.W., R.A., and I.M. performed the experiments. M.P.W., E.L.H, and D.N. analyzed the proteomics data. E.L.H., C.A.F., D.N., R.J.S., E.C.Y.W., G.W.G.W., P.J.L., and S.P.G. edited the manuscript. G.W.G.W., P.J.L., and S.P.G. supervised all research.

ACKNOWLEDGMENTS

We are grateful to Dr. Andrew Davison for assistance with the assembly of HCMV FASTA files; to Joao Paulo, Ryan Kunz, and Martin Wuehr for mass spectrometry and to Alexander Devaux for technical assistance. This work was supported by a Wellcome Trust Fellowship (093966/Z/10/Z) to M.P.W.; an MRC Project Grant and a Wellcome Trust Programme Grant (G1000236, WT090323MA) to G.W.G.W., P.T., and E.C.Y.W.; a Wellcome Trust Senior Fellowship (084957/Z/08/Z) to P.J.L. and National Institute of Health grant (GM067945) to S.P.G. This study was additionally supported by the Cambridge Biomedical Research Centre, UK. We have filed a provisional patent based on our findings.

Received: November 4, 2013
Revised: February 18, 2014
Accepted: April 3, 2014
Published: June 5, 2014

REFERENCES

Alexander, B.T., Hladnik, L.M., Augustin, K.M., Casabar, E., McKinnon, P.S., Reichley, R.M., Ritchie, D.J., Westervelt, P., and Dubberke, E.R. (2010). Use of cytomegalovirus intravenous immune globulin for the adjunctive treatment of cytomegalovirus in hematopoietic stem cell transplant recipients. Pharmacotherapy *30*, 554–561.

Alwine, J.C. (2012). The human cytomegalovirus assembly compartment: a masterpiece of viral manipulation of cellular processes that facilitates assembly and egress. PLoS Pathog. *8*, e1002878.

Amsler, L., Verweij, M.C., and DeFilippis, V.R. (2013). The tiers and dimensions of evasion of the type I interferon response by human cytomegalovirus. J. Mol. Biol. *425*, 4857–4871.

Angelova, M., Zwezdaryk, K., Ferris, M., Shan, B., Morris, C.A., and Sullivan, D.E. (2012). Human cytomegalovirus infection dysregulates the canonical Wnt/β-catenin signaling pathway. PLoS Pathog. *8*, e1002959.

Bonneville, M., O'Brien, R.L., and Born, W.K. (2010). Gammadelta T cell effector functions: a blend of innate programming and acquired plasticity. Nat. Rev. Immunol. *10*, 467–478.

Ceeraz, S., Nowak, E.C., and Noelle, R.J. (2013). B7 family checkpoint regulators in immune regulation and disease. Trends Immunol. *34*, 556–563.

Chambers, J., Angulo, A., Amaratunga, D., Guo, H., Jiang, Y., Wan, J.S., Bittner, A., Frueh, K., Jackson, M.R., Peterson, P.A., et al. (1999). DNA microarrays of the complex human cytomegalovirus genome: profiling kinetic class with drug sensitivity of viral gene expression. J. Virol. *73*, 5757–5766.

Duggal, N.K., and Emerman, M. (2012). Evolutionary conflicts between viruses and restriction factors shape immunity. Nat. Rev. Immunol. *12*, 687–695.

Dunn, C., Chalupny, N.J., Sutherland, C.L., Dosch, S., Sivakumar, P.V., Johnson, D.C., and Cosman, D. (2003a). Human cytomegalovirus glycoprotein UL16 causes intracellular sequestration of NKG2D ligands, protecting against natural killer cell cytotoxicity. J. Exp. Med. *197*, 1427–1439.

Feng, X., Schröer, J., Yu, D., and Shenk, T. (2006). Human cytomegalovirus pUS24 is a virion protein that functions very early in the replication cycle. J. Virol. *80*, 8371–8378.

Gariano, G.R., Dell'Oste, V., Bronzini, M., Gatti, D., Luganini, A., De Andrea, M., Gribaudo, G., Gariglio, M., and Landolfo, S. (2012). The intracellular DNA sensor IFI16 gene acts as restriction factor for human cytomegalovirus replication. PLoS Pathog. *8*, e1002498.

Hansen, S.G., Piatak, M., Jr., Ventura, A.B., Hughes, C.M., Gilbride, R.M., Ford, J.C., Oswald, K., Shoemaker, R., Li, Y., Lewis, M.S., et al. (2013). Immune clearance of highly pathogenic SIV infection. Nature *502*, 100–104.

Huang, W., Sherman, B.T., and Lempicki, R.A. (2009). Systematic and integrative analysis of large gene lists using DAVID bioinformatics resources. Nat. Protoc. *4*, 44–57.

Hubo, M., Trinschek, B., Kryczanowsky, F., Tuettenberg, A., Steinbrink, K., and Jonuleit, H. (2013). Costimulatory molecules on immunogenic versus tolerogenic human dendritic cells. Front Immunol *4*, 82.

Hunter, S., Jones, P., Mitchell, A., Apweiler, R., Attwood, T.K., Bateman, A., Bernard, T., Binns, D., Bork, P., Burge, S., et al. (2012). InterPro in 2011: new developments in the family and domain prediction database. Nucleic Acids Res. *40* (Database issue), D306–D312.

Huttlin, E.L., Jedrychowski, M.P., Elias, J.E., Goswami, T., Rad, R., Beausoleil, S.A., Villén, J., Haas, W., Sowa, M.E., and Gygi, S.P. (2010). A tissue-specific atlas of mouse protein phosphorylation and expression. Cell *143*, 1174–1189.

Khan, Z., Yaiw, K.C., Wilhelmi, V., Lam, H., Rahbar, A., Stragliotto, G., and Söderberg-Nauclér, C. (2014). Human cytomegalovirus immediate early proteins promote degradation of connexin 43 and disrupt gap junction communication: implications for a role in gliomagenesis. Carcinogenesis *35*, 145–154.

Kim, Y.E., Lee, J.H., Kim, E.T., Shin, H.J., Gu, S.Y., Seol, H.S., Ling, P.D., Lee, C.H., and Ahn, J.H. (2011a). Human cytomegalovirus infection causes degradation of Sp100 proteins that suppress viral gene expression. J. Virol. *85*, 11928–11937.

Koyuncu, E., Purdy, J.G., Rabinowitz, J.D., and Shenk, T. (2013). Saturated very long chain fatty acids are required for the production of infectious human cytomegalovirus progeny. PLoS Pathog. *9*, e1003333.

Le, V.T., Trilling, M., Wilborn, M., Hengel, H., and Zimmermann, A. (2008). Human cytomegalovirus interferes with signal transducer and activator of transcription (STAT) 2 protein stability and tyrosine phosphorylation. J. Gen. Virol. *89*, 2416–2426.

Ma, Y., Wang, N., Li, M., Gao, S., Wang, L., Zheng, B., Qi, Y., and Ruan, Q. (2012). Human CMV transcripts: an overview. Future Microbiol. *7*, 577–593.

McAlister, G.C., Huttlin, E.L., Haas, W., Ting, L., Jedrychowski, M.P., Rogers, J.C., Kuhn, K., Pike, I., Grothe, R.A., Blethrow, J.D., and Gygi, S.P. (2012). Increasing the multiplexing capacity of TMTs using reporter ion isotopologues with isobaric masses. Anal. Chem. *84*, 7469–7478.

Mocarski E.S., Shenk T., Griffiths P.D., and Pass R.F., eds. (2013). Cytomegaloviruses, 6th Edition (Philadelphia: Lipincott Williams and Wilkins).

Nichols, W.G., Corey, L., Gooley, T., Davis, C., and Boeckh, M. (2002). High risk of death due to bacterial and fungal infection among cytomegalovirus (CMV)-seronegative recipients of stem cell transplants from seropositive donors: evidence for indirect effects of primary CMV infection. J. Infect. Dis. *185*, 273–282.

Nikolov, D.B., Xu, K., and Himanen, J.P. (2013). Eph/ephrin recognition and the role of Eph/ephrin clusters in signaling initiation. Biochim. Biophys. Acta *1834*, 2160–2165.

Omoto, S., and Mocarski, E.S. (2014). Transcription of true late (γ2) cytomegalovirus genes requires UL92 function that is conserved among beta- and gammaherpesviruses. J. Virol. *88*, 120–130.

Paludan, S.R., Bowie, A.G., Horan, K.A., and Fitzgerald, K.A. (2011). Recognition of herpesviruses by the innate immune system. Nat. Rev. Immunol. *11*, 143–154.

Pease, B.N., Huttlin, E.L., Jedrychowski, M.P., Talevich, E., Harmon, J., Dillman, T., Kannan, N., Doerig, C., Chakrabarti, R., Gygi, S.P., and Chakrabarti, D. (2013). Global analysis of protein expression and phosphorylation of three stages of Plasmodium falciparum intraerythrocytic development. J. Proteome Res. *12*, 4028–4045.

Powers, C., DeFilippis, V., Malouli, D., and Früh, K. (2008). Cytomegalovirus immune evasion. Curr. Top. Microbiol. Immunol. *325*, 333–359.

Prod'homme, V., Sugrue, D.M., Stanton, R.J., Nomoto, A., Davies, J., Rickards, C.R., Cochrane, D., Moore, M., Wilkinson, G.W., and Tomasec, P. (2010). Human cytomegalovirus UL141 promotes efficient downregulation of the natural killer cell activating ligand CD112. J. Gen. Virol. *91*, 2034–2039.

Rahm, N., and Telenti, A. (2012). The role of tripartite motif family members in mediating susceptibility to HIV-1 infection. Curr Opin HIV AIDS *7*, 180–186.

Schoggins, J.W., Wilson, S.J., Panis, M., Murphy, M.Y., Jones, C.T., Bieniasz, P., and Rice, C.M. (2011). A diverse range of gene products are effectors of the type I interferon antiviral response. Nature *472*, 481–485.

Scott, I. (2009). Degradation of RIG-I following cytomegalovirus infection is independent of apoptosis. Microbes Infect. *11*, 973–979.

Stanton, R.J., McSharry, B.P., Rickards, C.R., Wang, E.C., Tomasec, P., and Wilkinson, G.W. (2007). Cytomegalovirus destruction of focal adhesions revealed in a high-throughput Western blot analysis of cellular protein expression. J. Virol. *81*, 7860–7872.

Stenberg, R.M., Depto, A.S., Fortney, J., and Nelson, J.A. (1989). Regulated expression of early and late RNAs and proteins from the human cytomegalovirus immediate-early gene region. J. Virol. *63*, 2699–2708.

Stern-Ginossar, N., Weisburd, B., Michalski, A., Le, V.T., Hein, M.Y., Huang, S.X., Ma, M., Shen, B., Qian, S.B., Hengel, H., et al. (2012). Decoding human cytomegalovirus. Science *338*, 1088–1093.

Subramanian, A., Tamayo, P., Mootha, V.K., Mukherjee, S., Ebert, B.L., Gillette, M.A., Paulovich, A., Pomeroy, S.L., Golub, T.R., Lander, E.S., and Mesirov, J.P. (2005). Gene set enrichment analysis: a knowledge-based approach for interpreting genome-wide expression profiles. Proc. Natl. Acad. Sci. USA *102*, 15545–15550.

Sullivan, R., Fassolitis, A.C., Larkin, E.P., Read, R.B., Jr., and Peeler, J.T. (1971). Inactivation of thirty viruses by gamma radiation. Appl. Microbiol. *22*, 61–65.

Takamatsu, H., and Kumanogoh, A. (2012). Diverse roles for semaphorin-plexin signaling in the immune system. Trends Immunol. *33*, 127–135.

Terhune, S.S., Moorman, N.J., Cristea, I.M., Savaryn, J.P., Cuevas-Bennett, C., Rout, M.P., Chait, B.T., and Shenk, T. (2010). Human cytomegalovirus UL29/28 protein interacts with components of the NuRD complex which promote accumulation of immediate-early RNA. PLoS Pathog. *6*, e1000965.

Ting, L., Rad, R., Gygi, S.P., and Haas, W. (2011). MS3 eliminates ratio distortion in isobaric multiplexed quantitative proteomics. Nat. Methods *8*, 937–940.

Tomasec, P., Wang, E.C., Davison, A.J., Vojtesek, B., Armstrong, M., Griffin, C., McSharry, B.P., Morris, R.J., Llewellyn-Lacey, S., Rickards, C., et al. (2005). Downregulation of natural killer cell-activating ligand CD155 by human cytomegalovirus UL141. Nat. Immunol. *6*, 181–188.

van der Wal, F.J., Kikkert, M., and Wiertz, E. (2002). The HCMV gene products US2 and US11 target MHC class I molecules for degradation in the cytosol. Curr. Top. Microbiol. Immunol. *269*, 37–55.

Varnum, S.M., Streblow, D.N., Monroe, M.E., Smith, P., Auberry, K.J., Pasa-Tolic, L., Wang, D., Camp, D.G., 2nd, Rodland, K., Wiley, S., et al. (2004). Identification of proteins in human cytomegalovirus (HCMV) particles: the HCMV proteome. J. Virol. *78*, 10960–10966.

Vavassori, S., Kumar, A., Wan, G.S., Ramanjaneyulu, G.S., Cavallari, M., El Daker, S., Beddoe, T., Theodossis, A., Williams, N.K., Gostick, E., et al. (2013). Butyrophilin 3A1 binds phosphorylated antigens and stimulates human $\gamma\delta$ T cells. Nat. Immunol. *14*, 908–916.

Vivier, E., Tomasello, E., Baratin, M., Walzer, T., and Ugolini, S. (2008). Functions of natural killer cells. Nat. Immunol. *9*, 503–510.

Weekes, M.P., Antrobus, R., Talbot, S., Hör, S., Simecek, N., Smith, D.L., Bloor, S., Randow, F., and Lehner, P.J. (2012). Proteomic plasma membrane profiling reveals an essential role for gp96 in the cell surface expression of LDLR family members, including the LDL receptor and LRP6. J. Proteome Res. *11*, 1475–1484.

Weekes, M.P., Tan, S.Y.L., Poole, E., Talbot, S., Antrobus, R., Smith, D.L., Montag, C., Gygi, S.P., Sinclair, J.H., and Lehner, P.J. (2013). Latency-associated degradation of the MRP1 drug transporter during latent human cytomegalovirus infection. Science *340*, 199–202.

Wilkinson, G.W., Tomasec, P., Stanton, R.J., Armstrong, M., Prod'homme, V., Aicheler, R., McSharry, B.P., Rickards, C.R., Cochrane, D., Llewellyn-Lacey, S., et al. (2008). Modulation of natural killer cells by human cytomegalovirus. J. Clin. Virol. *41*, 206–212.

Witherden, D.A., Watanabe, M., Garijo, O., Rieder, S.E., Sarkisyan, G., Cronin, S.J., Verdino, P., Wilson, I.A., Kumanogoh, A., Kikutani, H., et al. (2012). The CD100 receptor interacts with its plexin B2 ligand to regulate epidermal $\gamma\delta$ T cell function. Immunity *37*, 314–325.